

## Scaling of Shear-Induced Transformations in Membrane Phases

L. Porcar, W. A. Hamilton,\* and P. D. Butler

*Solid State Division, Oak Ridge National Laboratory, Oak Ridge, Tennessee 37831*

Gregory G. Warr

*School of Chemistry, The University of Sydney, Sydney, NSW 2006, Australia*

(Received 1 April 2002; published 24 September 2002)

Surfactant sponges are complex-fluid phases made up of convolutions of bilayer sheets. Although isotropic and free flowing they exhibit transient birefringence when stirred, reminiscent of the birefringence of lamellar phases. Previous attempts to understand this effect have led to confusing and often conflicting results. We have used a novel approach to designing the chemical system that gives us control over the relevant parameters needed to study microstructural and macroscopic responses of these phases to shear. We find a remarkable universal scaling behavior for both sponge and shear-induced lamellar states, which resolves a number of long-standing questions about these systems.

DOI: 10.1103/PhysRevLett.89.168301

PACS numbers: 82.70.Uv, 47.20.Hw, 61.12.Ex, 83.60.Rs

Surfactant molecules self-assemble in water to form a great variety of structures, including phases composed of extended flexible bilayer membranes [1]. These may display smectic order by stacking with a periodicity  $d$  as in the birefringent anisotropic lamellar  $L_\alpha$  phase, or they may form a meandering interface separating two interpenetrating labyrinths of solvent known as the “sponge” or  $L_3$  phase [2], in which the convolutions of the separating membrane define a pore or water channel with a characteristic size,  $\xi$ , inversely proportional to the membrane volume fraction,  $\phi$  (see Fig. 1).  $L_\alpha$  phases display complex rheological responses with multiple transitions due to bilayer alignments or the formation of mesoscale structures such as multilamellar vesicles [3–5]. In contrast, due to their flexible isotropic structure,  $L_3$  sponge phases, like the closely related bicontinuous microemulsions, typically display Newtonian flow behavior with low viscosities [6–8]. However, upon gentle shaking very dilute  $L_3$  samples display transient birefringence [9]. Because of the experimental challenges of studying these very dilute phases, the exact nature of this intriguing response has remained controversial [10–14].

The role of shear in inducing structural transitions in these structured but fluid phases is of particular interest as these systems are amenable to theories for free energy that can include shear. Cates and Milner [10] predicted that shear flow acting on an isotropic phase, such as a bicontinuous microemulsion or a sponge phase, will damp fluctuations normal to the flow velocity ( $V$ ) and velocity gradient ( $\nabla V$ ) directions, which may lead to the formation of lamellar structure with preferential bilayer orientation in the  $(V, \nabla V)$  plane (the “a” orientation). This transformation is essentially a quasithermodynamic perturbation of the equilibrium phase transition. Such an isotropic to lamellar transition has been reported in a diblock copolymer system [15].

When a sponge phase occurs in a surfactant phase diagram, it is always found adjacent to an  $L_\alpha$  phase and

is separated from it by only a very narrow coexistence region [16,17]. This, the transient birefringence of dilute sponge samples, and theoretical predictions have led to the expectation that sufficiently high shear should induce a similar lamellar bilayer alignment for these systems. The critical shear rate in a surfactant sponge should then obey the relationship [10]

$$\dot{\gamma}_c \sim \frac{k_B T}{\eta_s \xi^3} \sim \frac{k_B T}{\eta_s} \left(\frac{\phi}{\delta}\right)^3, \quad (1)$$

where  $k_B$  is the Boltzmann constant,  $T$  is absolute temperature,  $\eta_s$  is the viscosity of the solvent, and  $\delta$  is the membrane thickness. An aqueous sponge with  $\delta \sim 2$  nm and  $\phi \sim 0.10$  can therefore be expected to have a critical shear rate in excess of  $10^5$  s $^{-1}$ . Experimentally accessible critical shear rates, near or below  $10^3$  s $^{-1}$ , should occur for  $\phi < 0.02$ , and indeed transient birefringence is easily observed at these low concentrations. However, definitive structural determinations are very difficult, and the viscosity for such samples is too low for rheological measurements of the shear thinning expected with lamellar shear alignment to be practicable.

The system studied here consists of cetylpyridinium chloride (CPCl) plus hexanol as membrane-forming surfactants in a continuous solvent phase of heavy brine (0.2 M sodium chloride in D $_2$ O) containing dissolved

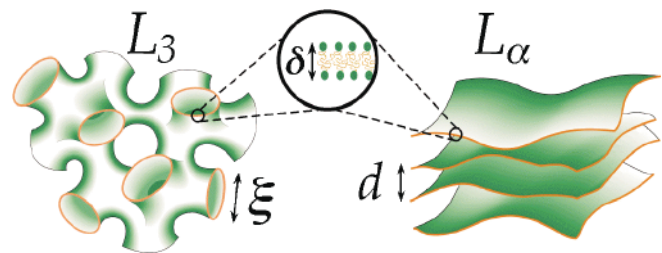


FIG. 1 (color).  $L_3$  and  $L_\alpha$  membrane morphologies and their respective characteristic dimensions  $\xi$ ,  $d$ , and  $\delta$ .

dextrose. The addition of dextrose at volume fractions in water,  $\psi_s$ , up to 0.4 allows us to vary the solvent phase viscosity between 1 and 13.6 cP, thus reducing the critical shear rates. Sugars have previously been shown to have little or no effect on the phase diagram of some microemulsions [18], and we similarly find only slight effects of the added dextrose on the phase diagram of the CPCl/hexanol/brine system. These are comparable to the effect of replacing H<sub>2</sub>O with D<sub>2</sub>O for contrast in our SANS measurements, indicating that the equilibrium membrane thickness and correlation length of the sponge phases is insensitive to added dextrose [19]. This tunable system allows us to present macroscopic rheological measurements in parallel with neutron scattering measurements of the microscopic structural response to shear flow.

Figure 2(a) shows the results of Couette rheometer measurements made at ORNL [20] on seven “sweetened” CPCl/hexanol/brine sponge phases with a range of membrane and dextrose volume fractions displayed against a rescaled shear rate  $\dot{\gamma}\eta_s/\phi^3$ . The scaling factor  $\eta_s/\phi^3$  varies by nearly 2 orders of magnitude for these samples ( $8.8 \times 10^3$ – $5.0 \times 10^5$ ) and clear master curve behavior demonstrates that the sponge phase shear response scales as predicted by Eq. (1). In the low shear region I these systems all show the constant viscosity Newtonian behavior typical of sponge phases. With increasing shear rates in a second region II the solutions shear thin dramatically with the viscosity falling by a factor of about 3. At higher shear rates our lower  $\phi$  highest  $\eta_s$  samples reach a third region III in which viscosity is once again constant. Also shown in Fig. 2(a) (right scale) are master curves of the scaled shear stress  $\tau/\phi^3$ . Note the absence of a plateau in these stress curves in the shear-thinning region II. This indicates that the transition observed here is not first order and rules out biphasic effects such as “shear banding” [21,22], distinguishing this response from that recently reported for a polymeric bicontinuous microemulsion [23].

Scattering measurements were performed using the ORNL Couette shear cell on the NG3 SANS spectrometer at the National Institute of Standards and Technology Center for Neutron Research [24]. These were performed with the incident beam radial and tangential to the sheared sample annulus (Fig. 3(a)) yielding scattering patterns in the flow/vorticity ( $V, Z$ ) and velocity gradient/vorticity ( $\nabla V, Z$ ) planes respectively. Figure 3(b) shows scattering measurements in both geometries over a range of shear rates for a low membrane volume fraction sponge phase sample with a high solvent viscosity, which shows the full range of scattering behavior we observed for these samples. In the low shear region I the scattering pattern is isotropic with a broad correlation ring peaking at  $Q_\xi = 2\pi/\xi$  characteristic of the sponge pore size. As the shear rate increases in region II, increasing shear rate yields increasing anisotropy in both scattering geometries. A sharp correlation peak develops in the  $\nabla V$  direction, indicating a smectic ordering of membranes normal

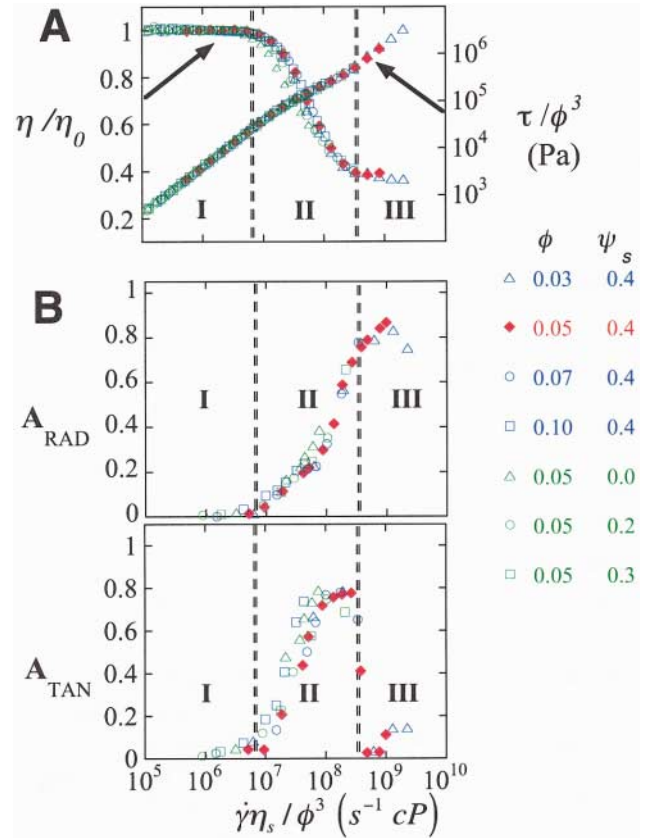


FIG. 2 (color). Master curve behavior versus rescaled shear rate  $\dot{\gamma}\eta_s/\phi^3$ . Open green symbols: constant  $\phi=0.05$  series; open blue symbols: constant  $\eta_s=13.6$  cP ( $\psi_s=0.4$ ) series; common member sample: solid red diamonds. (a) Scaled rheological data for a range of membrane volume fractions  $\phi$  and dextrose concentrations  $\psi_s$  (solvent viscosities  $\eta_s$ ). Viscosity normalized to the zero shear limit,  $\eta/\eta_0$  (left scale) and rescaled shear stress  $\tau/\phi^3$  (right scale). (b) Corresponding structural anisotropy parameters  $A_{\text{RAD}}$  and  $A_{\text{TAN}}$  from scattering measurements.

to the velocity gradient, i.e., parallel to the local flow/vorticity ( $V, Z$ ) plane (i.e., the “c” orientation). This intensity eventually saturates, but remains stable over only a narrow range of shear rates. At higher shears lower  $\phi$  highest  $\eta_s$  samples such as this one cross into region III where the alignment peak intensity falls rapidly and strong isotropic scattering emerges at low  $Q$  to dominate the final scattering pattern.

The structural response to all seven samples may be quantified in terms of the anisotropy of scattering intensities in perpendicular directions: For the radial geometry  $A_{\text{RAD}} \equiv (I_Z - I_V)/(I_Z + I_V)$  and for the tangential geometry  $A_{\text{TAN}} \equiv (I_Z - I_{\nabla V})/(I_Z + I_{\nabla V})$ , where we evaluate the intensities within  $\pm 10^\circ$  of the axes at the scattering vector of the sponge phase correlation peak. Plotted against the rescaled shear rate  $\dot{\gamma}\eta_s/\phi^3$  in Fig. 2(b), the anisotropies show a strong correspondence with the rheological response.

In the Newtonian isotropic sponge region I the scattering pattern anisotropy is zero for both scattering

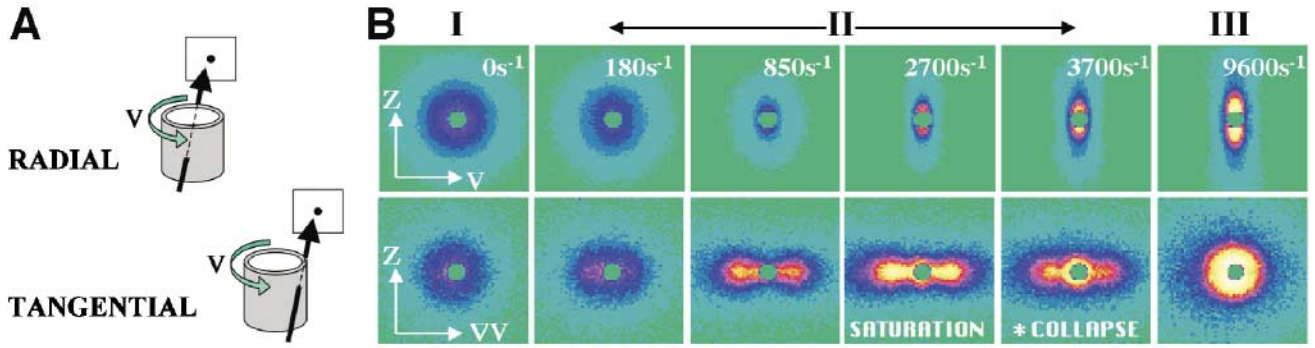


FIG. 3 (color). (a) Schematic of the beam incidence on the Couette SANS cell in radial and tangential geometries. (b) Scattering patterns in radial and tangential geometries for  $\phi = 0.05/\psi_s = 0.4$  ( $\eta_s = 13.6$  cP) sponge sample showing the full shear response.

geometries. In the shear-thinning region II, increasing anisotropy follows increasing rescaled shear rate in both scattering geometries, indicating the formation of an aligned lamellar phase. The development and eventual collapse of the aligned phase is further quantified in Fig. 4 which shows the variation in both peak position and intensity with shear rate for the two samples in our series for which region III is accessible and for which the correlation peak position can be accurately determined. As a direct consequence of the scale invariance of these membrane systems [2], this data may be conveniently plotted as a rescaled wave vector peak position  $Q_c/\phi$  and a rescaled correlation peak intensity  $I_c\phi$ . From this figure we see that like the anisotropy both  $Q_c/\phi$  and  $I_c\phi$  also increase gradually over this region, indicating a continuous process as membrane-forming material is excluded from channels and confined to oriented lamellar sheets. Consistent with the absence of a rheological stress plateau noted above, this progressive structural transformation clearly demonstrates that the transition cannot be first order. The total increase in  $Q_c/\phi$  is about 25%, from  $Q_\xi/\phi \sim 1.6 \text{ nm}^{-1}$  for the sponge correlation ring to  $Q_B/\phi \sim 2.0 \text{ nm}^{-1}$  for the final smectic Bragg peak. This is the same wave vector ratio as is observed between static SANS measurements of sponge and lamellar phases at the same membrane volume fraction [25].

At higher shears (but still well below the onset of turbulence) our lower  $\phi$  higher  $\eta_s$  samples cross into region III. Near the end of region II,  $\dot{\gamma}\eta_s/\phi^3 \approx 2 \times 10^8 \text{ s}^{-1} \text{ cP}$ ,  $A_{\text{RAD}}$  reaches a saturation value of about 0.8, which continues into region III. This is due to increasing scattering at low  $Q$  in the  $Z$  direction, with tails extending out to  $Q = Q_\xi$  overwhelming an almost total loss of scattering along the  $V$  direction. The variation of  $A_{\text{TAN}}$  is more dramatic. It has saturated within region II, also at about 0.8, for  $\dot{\gamma}\eta_s/\phi^3 \approx 7 \times 10^7 \text{ s}^{-1} \text{ cP}$ , due to Bragg scattering along  $\nabla V$  indicating nearly complete lamellar alignment. At the region III boundary ( $\dot{\gamma}\eta_s/\phi^3 \approx 4 \times 10^8 \text{ s}^{-1} \text{ cP}$ )  $A_{\text{TAN}}$  and the rescaled Bragg intensity  $I_c\phi$  fall sharply, though the rescaled peak position  $Q_c/\phi$  stays at the smectic Bragg value  $\sim 2.0 \text{ nm}^{-1}$ . Simultaneously strong isotropic scattering emerges at

low  $Q$  corresponding to correlations on length scales  $\gg \xi$  in the velocity gradient and vorticity directions. This dominates the final scattering patterns, indicating a collapse of the shear-induced lamellar phase.

The correspondence between our rheological and microstructural measurements leads us to the following interpretation of the shear response. In the Newtonian region I we observe no structural changes as the response frequency characterizing the dynamics of the membrane passages in the sponge phase is much greater than the applied shear rate. In region II when the shear rate approaches this frequency the density of connections or handles in the gradient direction ( $\nabla V$ ) decreases, leading to the development of smectic order in that direction. That this order develops in the so-called “c” orientation indicates that it is fluctuations in the gradient direction ( $\nabla V$ ) that are being suppressed rather than the vorticity ( $Z$ ) direction of the predicted “a” orientation. At shear rates high enough to totally eliminate the channels along  $\nabla V$  the intensity  $I_{\nabla V}$  saturates indicating the appearance of a fully aligned lamellar phase.

In region III, the induced lamellar phase collapses into a new structure. When undulation forces stabilize a lamellar structure it has been theoretically predicted that such a collapse should occur when shear suppresses fluctuations [26,27], but this has not previously been reported experimentally for a bulk equilibrium lamellar phase.

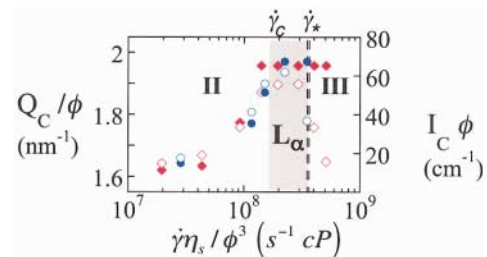


FIG. 4 (color). Rescaled correlation peak position  $Q_c/\phi$  (left scale, closed symbols) and intensity  $I_c\phi$  (right scale, open symbols) vs  $\dot{\gamma}\eta_s/\phi^3$  (regions II and III) for  $\phi = 0.05/\psi_s = 0.4$  (red) and  $\phi = 0.07/\psi_s = 0.4$  (blue) samples. Shaded:  $I_c\phi$  plateau of the saturated shear-induced  $L_\alpha$  signal.

This mechanism is a logical extension of the sponge-to-lamellar transition itself, which occurs by suppression of membrane fluctuations in the  $\nabla V$  direction in the isotropic phase. Lamellar collapse was predicted by Ramaswamy [26] for shear rates larger than a critical value  $\dot{\gamma}_* \sim (k_B T)^3 / \kappa^2 \eta_s d^3$ , where  $\kappa$  is the membrane's bending modulus and  $d$  is the separation of adjacent bilayers. For CPCI-hexanol membranes  $\kappa$  has been experimentally determined at room temperature [25,28,29] to be  $\approx 1k_B T$ , so we have  $\dot{\gamma}_* \sim k_B T / \eta_s d^3$ . This critical shear rate follows the same scaling dependence as  $\dot{\gamma}_c$ , but with a different characteristic distance. Since  $d = 2\pi/Q_B$  and assuming a rough equality of the respective prefactors we might expect  $\dot{\gamma}_*/\dot{\gamma}_c \sim (\xi/d)^3 = (Q_B/Q_\xi)^3$ . For our observed scattering peaks  $Q_B/Q_\xi \approx 1.25$ , so  $\dot{\gamma}_*/\dot{\gamma}_c \sim 2$ . This is close to the width of the stable region we observe for the saturated shear-induced lamellar phase before it collapses at higher shear (the shaded  $I_c \phi$  plateau region in Fig. 4). In respect of the narrowness of this window of stability, we note that Bruinsma and Rabin [27] speculated that lamellar collapse might preclude the shear-induced sponge-to-lamellar transformation altogether. Further measurements are required to establish the nature of the collapse and of the large scale correlations giving rise to the observed scattering in this high shear region.

While the magnitude of the critical shear rates and the scaling behavior of the shear response we observe are as predicted by Cates and Milner (as might also be expected from simple membrane diffusion or dimensional arguments), this is not the case for either the nature of the transition nor the direction of the smectic orientation. We observe "c" orientation of the shear-induced lamellar phase rather than the predicted "a," which is also consistent with previous work on very dilute sponge phases of the nonionic surfactant  $C_{12}E_5$  under oscillatory shear [11]. Further, Cates and Milner predicted only a weakening of the first order nature of the transition. No evidence of a biphasic region indicating first order character was apparent in either our rheological or structural measurements. Rather they show that the transformation of the sponge phase to the shear-induced lamellar phase is a continuous higher order process. While the theory has been confirmed for some isotropic copolymer phases [15], our observations and varying details of shear responses from other topologically similar systems with differing relaxation paths [23] suggest that in its present form it is not straightforwardly applicable to the class as a whole. A more sophisticated model is required to fully explain the shear responses of these sponge systems. On the other hand, these results offer a first confirmation of the predictions of Ramaswamy and of Bruinsma and Rabin regarding the collapse of lamellar phases at high shear and nicely answer the question of the latter regarding the stability of a shear-induced lamellar phase.

Our thanks go to Gregoire Porte for fruitful discussions; Costas Tsouris for the use of his rheometer,

D. Glandon and B. Taylor for their work on the ORNL Couette shear cell; M. Lumsden and M. Yethiraj of ORNL; and Jean Pierre Fluxench for Fig. 1. The NG3 SANS instrument is operated by the NIST, U.S. Department of Commerce, with funding from the U.S. National Science Foundation under Agreement No. DMR-9986442. ORNL is managed by UT-Battelle LLC for the U.S. Department of Energy under Contract No. DE-AC05-00OR22725. G.G.W. acknowledges Australian Nuclear Science and Technology Organization and Australian Research Council support.

\*Corresponding author: HamiltonWA@ornl.gov

- [1] S.T. Hyde, *The Language of Shape* (Elsevier Science, Amsterdam, 1997).
- [2] G. Porte, *J. Phys. Condens. Matter* **4**, 8649 (1992), and references therein.
- [3] O. Diat, D. Roux, and F. Nallet, *J. Phys. II (France)* **3**, 1427 (1993).
- [4] O. Diat and D. Roux, *J. Phys. II (France)* **3**, 9 (1993).
- [5] J. Zipfel *et al.*, *J. Phys. Chem. B* **103**, 2841 (1999).
- [6] P. Snabre and G. Porte, *Europhys. Lett.* **13**, 641 (1990).
- [7] C.-M. Chen and G.G. Warr, *J. Phys. Chem.* **96**, 9492 (1992).
- [8] M.R. Anklam, R.K. Prudhomme, and G.G. Warr, *AIChE J.* **41**, 677 (1995).
- [9] O. Diat and D. Roux, *Langmuir* **11**, 1392 (1995).
- [10] M.E. Cates and S.T. Milner, *Phys. Rev. Lett.* **62**, 1856 (1989).
- [11] J. Yamamoto and H. Tanaka, *Phys. Rev. Lett.* **77**, 4390 (1996).
- [12] H.F. Mahjoub *et al.*, *Phys. Rev. Lett.* **81**, 2076 (1998).
- [13] A. Leon *et al.*, *Phys. Rev. Lett.* **86**, 938 (2001).
- [14] P.D. Butler *et al.*, *Phys. Rev. Lett.* **88**, 059601 (2002).
- [15] K.A. Koppi, M. Tirrell, and F.S. Bates, *Phys. Rev. Lett.* **70**, 1449 (1993).
- [16] G. Porte *et al.*, *J. Phys. (Paris)* **49**, 511 (1988).
- [17] Y. Nastishin, E. Lambert, and P. Boltenhagen, *C. R. Acad. Sci. Ser. Gen., Ser. IIb* **321**, 205 (1995).
- [18] V. Chen, Ph.D. thesis, University of Minnesota, 1988.
- [19] L. Porcar *et al.* (to be published).
- [20] Haake RheoStress RS150 with double gap cylinder sensor DG41 (Gebr. Haake GmbH, Karlsruhe, Germany).
- [21] J.F. Berret, D.C. Roux, and P. Lindner, *Eur. Phys. J. B* **5**, 67 (1998).
- [22] P.D. Olmsted and C.Y.D. Lu, *Phys. Rev. E* **56**, R55 (1997).
- [23] K. Krishnan *et al.*, *Phys. Rev. Lett.* **87**, 098301 (2001); *J. Rheol. (N.Y.)* **46**, 529 (2002).
- [24] L. Porcar *et al.*, *Rev. Sci. Instrum.* **73**, 2345 (2002).
- [25] W.A. Hamilton *et al.*, *J. Chem. Phys.* **116**, 8533 (2002).
- [26] S. Ramaswamy, *Phys. Rev. Lett.* **69**, 112 (1992).
- [27] R. Bruinsma and Y. Rabin, *Phys. Rev. A* **45**, 994 (1992).
- [28] G. Bouglet *et al.*, *Phys. Rev. E* **57**, 834 (1998).
- [29] D. Roux *et al.*, *Europhys. Lett.* **17**, 575 (1992).